

NARROW SPECTRAL BANDWIDTH OPTIMIZATION OF COMPTON SCATTERING SOURCES*

F. Albert[†], S.G. Anderson, S.M. Betts, R.R. Cross, G. Deis, C.A. Ebberts, D.J. Gibson, T.L. Houck, R.A. Marsh, M. Messerly, S.S. Wu, C.W. Siders, C.P.J. Barty and F.V. Hartemann, LLNL, Livermore, CA, 94550, USA

Abstract

This paper presents the theoretical and numerical design and optimization of Mono-Energetic Gamma-Ray (MEGa-Ray) Compton scattering sources. A new precision source with up to 2.5 MeV photon energies, enabled by state-of-the-art laser and x-band linac technologies, is currently being built at LLNL. The theoretical design, which includes spectral bandwidth optimization and nonlinear effects, is presented. We review the potential sources of spectral broadening, in particular due to the electron beam properties. A three dimensional analytical model and numerical benchmarks have been developed to model the source characteristics based on given laser and electron beam distributions, including nonlinear spectra. Since MEGa-ray sources are being developed for precision applications such as nuclear resonance fluorescence, assessing spectral broadening mechanisms is essential.

INTRODUCTION

Nuclear Resonance Fluorescence (NRF) [1] is an isotope specific process in which a nucleus, excited by gamma-rays, radiates high energy photons at a specific energy. This process has been well known for several decades, and has potential high impact applications in homeland security, nuclear waste assay, medical imaging and stockpile surveillance, among other areas of interest. Although several successful experiments have demonstrated NRF detection with broadband bremsstrahlung gamma-ray sources [2], NRF lines are more efficiently detected when excited by narrowband gamma-ray sources. Indeed, the effective width of these lines, $\Delta E/E$, is on the order of 10^{-6} . Currently, Compton scattering is the only physical process capable of producing a narrow bandwidth radiation (below 1%) at gamma-ray energies, with state-of-the art accelerator and laser technologies. In Compton scattering sources, a short laser pulse and a relativistic electron beam collide to yield tunable, monochromatic, polarized gamma-ray photons. Several projects have recently utilized Compton scattering to conduct NRF experiments: Duke university [3], Japan [4] and Lawrence Livermore National Laboratory (LLNL) [5, 6, 7]. In particular, LLNL's Thomson-Radiated Extreme X-rays (T-REX) project demonstrated

isotope specific detection of low density materials behind heavier elements [5].

This paper presents, within the context of NRF-based applications, the theoretical and conceptual design of a narrowband monoenergetic gamma-ray (MEGa-ray) source. In particular, we investigate broadening mechanisms due to the electron beam distribution.

COMPTON SCATTERING: BASIC PRINCIPLES

The Compton formula can be derived from energy-momentum conservation, and expressed as follows:

$$u_\mu + \lambda k_\mu = v_\mu + \lambda q_\mu \quad (1)$$

Here, u_μ and v_μ are the initial and scattered electron 4-velocities, while k_μ and q_μ are the incident and scattered 4-wavenumbers, respectively. The 4-velocities are normalized, with $u_\mu u^\mu = v_\mu v^\mu = 1$, and the dispersion relation implies that $k_\mu k^\mu = q_\mu q^\mu = 0$. Hence, using these conditions allows for the elimination of the scattered electron 4-velocity, and results in:

$$u_\mu(k^\mu - q^\mu) = \lambda k_\mu q^\mu. \quad (2)$$

Eq. 2 can be also written in a slightly different manner by introducing the incident and scattered light-cone variables [10], $\kappa = u_\mu k^\mu$, and $\lambda = u_\mu q^\mu$, respectively:

$$\kappa - \lambda = \lambda k_\mu q^\mu. \quad (3)$$

Finally, in regular units and 3-vector form: $u_\mu = (\gamma, \mathbf{u})$; $q_\mu = q(1, \mathbf{n})$, where \mathbf{n} is the unit vector along the direction of observation; and $k_\mu = (k, \mathbf{k})$; this yields the well-known Compton formula:

$$\frac{q}{k} = \frac{\gamma - \mathbf{u} \cdot (\mathbf{k}/k)}{\gamma - \mathbf{n} \cdot \mathbf{u} + \lambda(k - \mathbf{n} \cdot \mathbf{k})}. \quad (4)$$

Here k is the wave number and $\gamma = 1/\sqrt{1 - v^2/c^2}$ is the electron relativistic factor. In other words:

$$\frac{q}{k} = \frac{\gamma - u \cos \varphi}{\gamma - u \cos \theta + \lambda k [1 - \cos(\theta + \varphi)]}, \quad (5)$$

where φ is the angle between the incident laser and electron and θ is the angle between the incident electron and scattered gamma-ray photon.

* This work performed under the auspices of the U.S. Department of Energy by Lawrence Livermore National Laboratory under Contract DE-AC52-07NA27344.

[†] albert6@llnl.gov

For realistic laser-electron interactions, one has to take into account the electron phase space and the laser transverse dimensions. The exact nonlinear plane wave solution for the 4-velocity has been derived in earlier work [11, 12, 13]:

$$u_\mu = u_\mu^0 + A_\mu - k_\mu \frac{A_\nu(A^\nu + 2u_0^\nu)}{2k_\nu u_0^\nu}, \quad (6)$$

where u_μ^0 is the initial 4-velocity and A_μ is the laser 4-potential. By using the nonlinear 4-velocity in conjunction with Eq. 2, one obtains:

$$\left(u_\mu^0 + A_\mu - k_\mu \frac{A_\nu A^\nu + 2u_\nu^0 A^\nu}{2u_\nu^0 k^\nu} \right) (k^\mu - q^\mu) = \lambda k_\mu q^\mu, \quad (7)$$

which, after applying the Lorentz gauge condition $k_\mu A^\mu = 0$, and the dispersion relation in vacuum, $k_\mu k^\mu = 0$, simplifies to:

$$u_\mu^0 k^\mu - \left(u_\mu^0 - \frac{k_\mu}{2u_\nu^0 k^\nu} \langle A_\nu A^\nu \rangle \right) q^\mu = \lambda k_\mu q^\mu. \quad (8)$$

This new relation is a modified form of the Compton formula, now including the nonlinear ponderomotive force of the laser field. When referring to the geometry described in Fig. 1, Eq. 8 becomes:

$$\frac{q}{k} = \frac{\gamma - u \cos(\epsilon + \varphi)}{\gamma - u \cos(\theta + \epsilon) + (1 - \cos(\varphi + \theta + \epsilon)) \left[\frac{\langle -A_\mu A^\mu \rangle}{2[\gamma - u \cos(\varphi + \epsilon)]} + \lambda k \right]}. \quad (9)$$

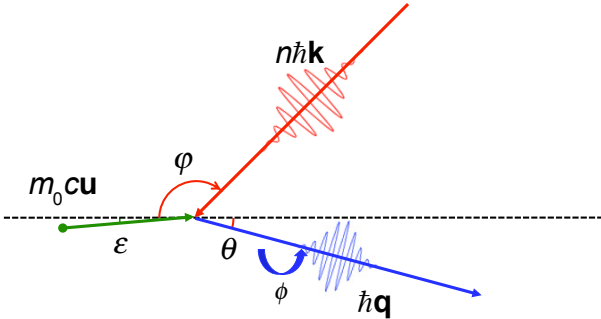


Figure 1: Definition of the Compton scattering geometry in the case of an electron beam.

Here the small angle ϵ is different for each electron and represents the emittance of the electron beam. Note also that $\langle -A_\mu A^\mu \rangle$ is the nonlinear radiation pressure. By looking at the variation of q as a function of all the parameters in Eq. 9, for on-axis observation ($\theta = 0$) one finds that $\Delta q/q \propto \Delta k/k$, $\Delta q/q \propto -\frac{1}{4} \Delta \varphi^2$, $\Delta q/q \propto 2 \Delta \gamma/\gamma$, $\Delta q/q \propto -\gamma^2 \Delta \epsilon^2$, and $\Delta q/q \propto -\frac{\Delta A^2}{1+A^2}$. While the gamma ray spectral width depends directly on the electron and laser energy spreads, it is also strongly affected by the electron beam emittance because of the γ^2 factor. This provides a

02 Synchrotron Light Sources and FELs

A14 Advanced Concepts

quick overview of the various sources of spectral broadening in a Compton scattering light source. Note that the negative variations are asymmetric broadening toward lower photon energies.

GAMMA-RAY SIMULATIONS

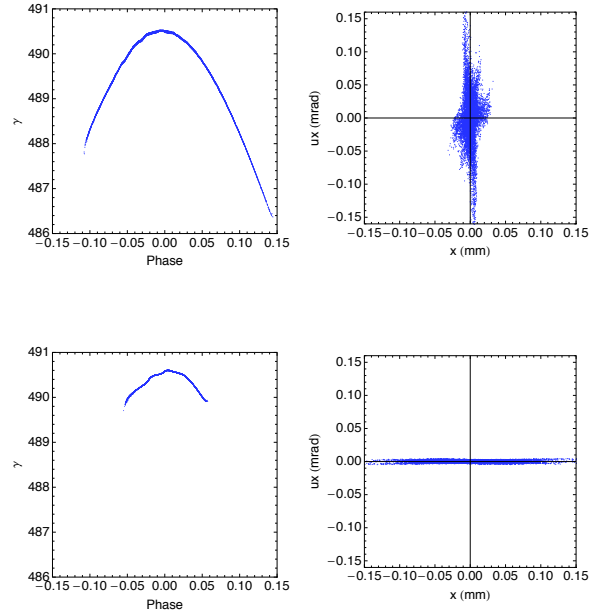


Figure 2: Electron beam distribution for a 250 pC (top) and 25 pC (bottom) electron beam. Shown are the energy (γ) vs. rf phase in radians (left) and the one dimensional phase space (right) on identical scales.

The spectral broadening mechanisms described above were explained from very basic Compton scattering theory. We have also developed a full three dimensional (3D) code to calculate gamma-ray spectra from real electron beam distributions and laser temporal and spatial profiles. Because the laser pulses are long enough compared to one optical cycle, the code uses a slowly varying envelope approximation. Paraxial, and weakly nonlinear approximations to develop a local plane-wave model leading to analytical expressions for the electron trajectories are also used. This code has been benchmarked against numerical simulations and showed excellent agreement throughout [13]. We have used the code and models described in details in [12, 13] to investigate spectral broadening, mainly due to the electron beam. Electron beam distributions were calculated using PARMELA. PARMELA uses macro-particles to represent the electron bunch and time steps to push particles. In our simulations 2-dimensional maps of the radio-frequency fields of the accelerator cavities were modeled with the SUPERFISH code and imported into the particle tracker. The space-charge forces are computed using a quasi-static ap-

proximation by transforming into a co-moving reference frame and computing and applying the Coulomb field on a mesh. For simulations presented in this paper, 10,000 macro-particles were used. Although simulations with up to 100,000 particles have been performed, this number was chosen to reduce our calculation duration, while providing the required resolution for the Compton scattering calculation. It was also much greater than the required number of particles to insure accurate modeling of the electron beam propagation through the accelerator. Fig. 2 shows two such distributions for a high charge (250 pC) and low charge (25 pC) electron beam. The high charge beam has a 0.35 mm.mrad emittance and a 0.17 % energy spread and the low charge beam has a 0.1 mm.mrad emittance and a 0.03 % energy spread. The rms focal spot sizes are respectively 13 μm and 36 μm . Both simulations include thermal emittance effects.

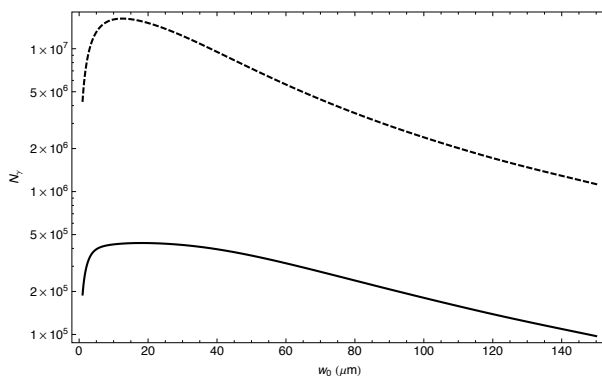


Figure 3: Total gamma-ray flux for a laser interacting with the high charge (dashed) and low charge (solid) electron beam. The laser parameters are: 10 ps FWHM pulse duration, 532 nm wavelength, 150 mJ energy.

Both electron beam distributions displayed in Fig. 2 have been used to calculate the total gamma-ray flux in the beam and gamma-ray spectra. Both calculations were performed with the recently published weakly nonlinear model and code [12, 13]. The flux, in Fig. 3, is plotted versus the laser beam waist, w_0 . Note that while identical laser parameters were used for the low charge and high charge electron beam, further optimization might yield to different optimal laser parameters for these two cases. The resulting normalized gamma-ray spectra, calculated using the optimal w_0 value, are displayed in Fig. 4.

CONCLUSION

We presented the theoretical design of narrow-band Compton scattering gamma-ray sources within the specific context of nuclear resonance fluorescence applications. NRF is a very powerful isotope-specific process that has potential high impact applications in homeland security, nuclear waste assay and management, stockpile

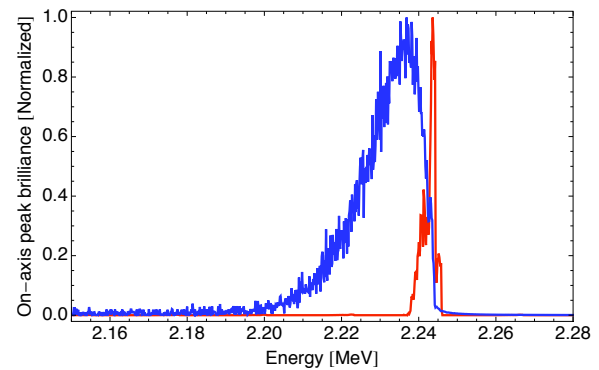


Figure 4: Normalized gamma-ray spectra for the 250 pC (blue) and 25 pC electron beam. The laser parameters are: 10 ps FWHM pulse duration, 532 nm wavelength, 150 mJ energy. The beam waist w_0 was chosen to yield the highest flux

surveillance or medicine. In order for this process to be fully efficient, it is necessary to operate in a spectrally narrow regime. In order to assess spectral broadening mechanisms in Compton scattering, detailed theory modeling are necessary. Our codes and models include an exhaustive description of electron beam properties as well as weakly nonlinear effects.

REFERENCES

- [1] U. Kneissl, H.M. Pitz and A. Zilges, Prog. Part. Nucl. Phys., 37, pp 349-433 (1996).
- [2] W. Bertozzi, *et al.*, Phys. Rev. C, 78, 041601(R) (2008).
- [3] C.A. Hagmann, *et al.*, J. Appl. Phys. 106, 084901 (2009).
- [4] N. Kikuzawa, *et al.*, Appl. Phys. Express 2, 036502 (2009).
- [5] F. Albert, *et al.*, Opt. Lett, 35, 3 354 (2010).
- [6] D. J. Gibson, *et al.*, Phys. Rev. ST Accel. Beams 13, 070703 (2010).
- [7] F. Albert, *et al.*, Phys. Rev. ST Accel. Beams 13, 070704 (2010).
- [8] W. Bertozzi, *et al.*, Nucl. Instrum. Methods Phys. Res. B 261, 331 (2007).
- [9] J. Pruet, *et al.*, J. Appl. Phys. 99, 123102 (2006).
- [10] L.M. Brown and R.P. Feynmann, Phys. Rev. 85, 231 (1952).
- [11] J.W. Meyer, Phys. Rev. D, 3, 621 (1971).
- [12] F.V. Hartemann, F. Albert, C.W. Siders and C.P.J. Barty, Phys. Rev. Lett., 105, 130801 (2010).
- [13] F. Albert, S.G. Anderson, D.J. Gibson, R.A. Marsh, C.W. Siders, C.P.J. Barty and F.V. Hartemann, Phys. Plasmas, 18, 013108 (2011).